

Cathode-sheath model for field emission sustained atmospheric pressure discharges

Cite as: Phys. Plasmas **28**, 033506 (2021); <https://doi.org/10.1063/5.0035710>

Submitted: 02 November 2020 . Accepted: 22 February 2021 . Published Online: 16 March 2021

 E. Cejas,  L. Prevosto,  F. O. Minotti,  M. Ferreyra,  J. C. Chamorro, and  B. Fina



View Online



Export Citation



CrossMark



Physics of Plasmas
Features in Plasma Physics Webinars

Register Today!

Cathode-sheath model for field emission sustained atmospheric pressure discharges

Cite as: Phys. Plasmas **28**, 033506 (2021); doi: [10.1063/5.0035710](https://doi.org/10.1063/5.0035710)

Submitted: 2 November 2020 · Accepted: 22 February 2021 ·

Published Online: 16 March 2021



View Online



Export Citation



CrossMark

E. Cejas,¹  L. Prevosto,^{2,a)}  F. O. Minotti,^{3,4}  M. Ferreyra,¹  J. C. Chamorro,¹  and B. Fina² 

AFFILIATIONS

¹Grupo de Descargas Eléctricas, Departamento Ing. Electromecánica, Facultad Regional Venado Tuerto (UTN), Laprida 651, Venado Tuerto 2600, Santa Fe, Argentina

²Facultad Regional Venado Tuerto, Departamento Ing. Electromecánica, Grupo de Descargas Eléctricas, Universidad Tecnológica Nacional, CONICET, Laprida 651, Venado Tuerto 2600, Santa Fe, Argentina

³Facultad de Ciencias Exactas y Naturales, Departamento de Física, Universidad de Buenos Aires, Buenos Aires 1428, Argentina

⁴Instituto de Física del Plasma (INFIP), CONICET-Universidad de Buenos Aires, Buenos Aires 1428, Argentina

^{a)}Author to whom correspondence should be addressed: prevosto@waycom.com.ar

ABSTRACT

The cathode-sheath region of a discharge in atmospheric pressure air with a flat copper cathode is numerically investigated by using a simple fluid model that takes into account non-local ionization. The effects of the cathode temperature are considered. Results are obtained in a wide current density range of $1\text{--}10^2$ A/cm², which spans from normal glow discharge, through abnormal glow discharge, up to the early stages of the arcing transition. It is shown that the glow-to-arc transition arises from a field-emission instability at the cathode when the current density is larger than ~ 10 A/cm², i.e., when the cathode field exceeds a critical value of about 45 V/ μ m for the conditions considered. It is also shown that the cathode temperature significantly influences the cathode-sheath region. The proposed model is validated by comparing the numerical results with available experimental data.

Published under license by AIP Publishing. <https://doi.org/10.1063/5.0035710>

I. INTRODUCTION

Measurements of cathode-sheath voltages in atmospheric pressure glow discharges^{1,2} suggest that secondary electron emission can still sustain the large (nearly quadratic³) increase in the cathode current density due to the increased pressure. However, such a state is unstable. A rise in the cathode current density above some critical value results, as a rule, in the glow-to-arc transition^{3,4} characterized by a large drop in the cathode-sheath voltage. This voltage drop is associated with a shift in the electron emission mechanism from secondary emission to field emission in cold cathodes.⁴ Gas discharge instabilities resulting in the plasma filamentation have been extensively studied, as summarized in a recent review article.⁵ However, there have not been many works characterizing the process within the cathode sheath, leading to an instability in the glow discharge.⁶ Note that for gaps below 10 μ m (i.e., field emission sustained microdischarges⁷) the glow regime is usually absent, even at atmospheric pressure, because the cathode-sheath thickness is typically higher than the gap length.⁴ In such a case, field emission in microdischarges leads to a direct transition from Townsend-to-arc discharge.⁸

In this work, a simple model of the cathode-sheath region of an atmospheric pressure air discharge with a cold cathode is presented. The model aims to study the elementary processes within the cathode sheath responsible for the glow-to-arc transition in which the field electron emission replaces secondary emission due to the increase in current density. The current density–voltage characteristic of the cathode sheath is presented over a wide range of current density values, from 1 to 10^2 A/cm². The proposed model is validated by comparing its numerical results with available experimental data.

II. CATHODE-SHEATH MODEL

A simple fluid model of the cathode sheath for a discharge in atmospheric pressure air with a flat Cu cathode is proposed. If the current density is low enough (i.e., well below that needed for an arc hot spot in Cu), the current is concentrated in a single spot causing a negligible erosion of the cathode surface, and no electrode material (metal vapor) is introduced into the discharge. The background gas temperature is assumed to be $T = 700$ K, i.e., close to that of the cathode spot. The temperature in current spots on Cu (which are not the hot arc

spots), at moderate and high-pressure discharges, typically does not exceed 700 K.⁹ The cathode sheath is assumed to be planar and one-dimensional. The reasons for this are that if the discharge current is not too low, at moderate and high-pressures, the current spot in the cathode has linear dimensions that are large compared to the sheath thickness.⁴

The electric field in the cathode sheath decreases almost linearly with the distance x from the cathode, becoming relatively small at the edge of the plasma, so that as a reasonable approximation we assume that^{4,7,10,11}

$$E(x) = E_C \left(1 - \frac{x}{d}\right), \quad (1)$$

where E_C is the field value at the cathode and d is the sheath thickness. It is expected that this assumption is not critical to the proposed model, particularly close to the cathode-sheath edge, because the mean electron energy in this region is well decoupled from the local field value. Both E_C and d depend on the nature and density of the gas and on the electron emission mechanism of the cathode surface. According to Poisson's equation, the positive space-charge density n_+ remains constant over the cathode sheath for the field distribution (1). It, thus, follows that⁶

$$\frac{E_C}{d} = \frac{e}{\epsilon_0} n_+ = \frac{1}{\epsilon_0} \left(\frac{j_+(0)}{v_+(0)}\right), \quad (2)$$

where $j_+(0)$ and $v_+(0)$ are the ion current density and ion drift velocity at the cathode surface, respectively, e is the absolute value of the electron charge, and ϵ_0 is the dielectric permittivity of vacuum. The number density of electrons in Poisson's equation is neglected because of their high mobility.⁴ Two sorts of positive ions are taken into account in the model, N_2^+ and O_2^+ ions. Reactions other than direct electron-impact ionization of air molecules are not considered. In high-field conditions, the ion drift velocity depends both on T and on the local reduced field.¹² Tabulated data¹³ for the momentum-transfer collision integral, extrapolated to the high-energy range through experimental data,¹⁴ are used in the calculations.

In order to include the effects of field emission at high-current density values, the ion current density at the cathode is given by

$$j_+(0) = \frac{j - j_{FN}}{1 + \gamma}, \quad (3)$$

where j is the total current density, γ is the secondary emission coefficient (taken to be 0.005 for air ions on an oxidized copper cathode⁴), and j_{FN} is the field emission current density given by the Fowler–Nordheim equation,¹⁵

$$j_{FN} = \frac{A_{FN} \beta^2 E_C^2}{\phi t^2(y)} \exp\left(-\frac{B_{FN} \phi^{\frac{3}{2}} v(y)}{\beta E_C}\right), \quad (4)$$

where A_{FN} and B_{FN} are constants, ϕ is the cathode work function (taken to be 2 eV, for the oxidized copper cathode⁴), and β is the field enhancement factor depending on the roughness of the emitting surface⁴ (taken from Ref. 15; see discussion in Sec. III). $v(y)$ and $t^2(y)$ are correction terms.¹⁶

To partly take account of non-local effects in the cathode sheath,¹⁷ the model also solves the electron energy equation,^{11,18}

$$\frac{d}{dx} \epsilon = E - (\epsilon + EI)\alpha - \sum_k \Delta \epsilon_k \delta_k, \quad (5)$$

where ϵ is the mean electron energy (in eV units). The second term on the right-hand side of (5) describes the electron energy spent in ionization processes and thermalization of the created electron (EI is the ionization energy per ionization event, equal to 15.6 eV for N_2 and 12.1 eV for O_2). The last term accounts for the electron energy transferred to molecules in high-threshold excitation reactions k . Excitation reactions with an energy threshold of $\Delta \epsilon_k \geq 9.97$ eV are considered in the calculations. It was found that the inclusion of other excitation reactions with lower energy threshold does not significantly affect the energy of the electrons under the high-field conditions considered. The Townsend ionization coefficients and the excitation coefficients are calculated as a function of ϵ for the mixture N_2 –20% O_2 , by solving the electron Boltzmann equation with the help of the Bolsig+ code.¹⁹ The corresponding cross-sectional data are taken from Ref. 20. A recent analysis reveals that the present approach (for which the electron transport coefficients and the excitation rates are determined as functions of electron energy rather than the local field, as was suggested in Ref. 21) is appropriate to model the cathode-sheath region of a glow discharge.²² When solving (5), it is assumed that the electrons are emitted from the cathode with a kinetic energy of about 1 eV.¹⁸

Moreover, the growth of the electron current density j_e over the cathode sheath is given by the multiplication factor M ,

$$M \equiv \exp\left(\int_0^d \alpha dx\right). \quad (6)$$

Neglecting the weak ion current entering the cathode sheath from the plasma side, the cathode sheath can be considered as an autonomous system;⁴ therefore, the condition of self-sustainment of current should be satisfied,

$$M = \frac{j(1 + \gamma)}{j\gamma + j_{FN}}. \quad (7)$$

Note that Eqs. (2)–(4) establish a relationship between E_C , d , and $v_+(0)$, for a given value of the total current density j . For a gas with only one type of ion, $v_+(0)$ depends only on T and the local reduced field (E_C/n , with n being the gas number density). In this case, by assuming a value of E_C and substituting it into (2), d is obtained [as $j_+(0)$ and $v_+(0)$ are completely defined by E_C]. Next, substituting $E(x)$ into (5), the distribution of $\epsilon(x)$ along the cathode layer is calculated, from which $\alpha(x)$ is, in turn, obtained. Then, substituting $\alpha(x)$ into the right side of (6), that is also the right side of (7), M is obtained by numerical integration. Finally, by comparing M with the value on the right side of (7), E_C is determined through an iterative process. Finally, using

$$V_C = \frac{E_C d}{2}, \quad (8)$$

the corresponding voltage drop across the cathode sheath V_C is obtained for the given value of j . On the other hand, if multiple ions are considered, an explicit relationship between d and E_C cannot be obtained. The reason is that $v_+(0)$ depends not only on the local field E_C but also on the ion composition at the cathode, which is determined by the ionization processes throughout the sheath,

$$v_+(0) = \sum \chi_i v_{+,i}(0), \tag{9}$$

where the mole fraction of ions of type i at the cathode χ_i is given by

$$\chi_i \equiv \frac{n_{+,i}(0)}{n_+} = \frac{1}{n_+ v_{+,i}(0)} \int_0^d \alpha_{ij} v_e dx, \tag{10}$$

where $n_{+,i}(0)$ and $v_{+,i}(0)$ refer to the number density and drift velocity of the ions of type i , at the cathode, respectively. α_i is the Townsend ionization coefficient of the corresponding reaction. In this case, in addition to assuming a value of E_C for a given current density of j , a starting value of χ_i must also be assumed. The above process is repeated, but the value of χ_i is then recalculated through (9) in each iteration. However, the iteration procedure has a rapid convergence because the value of χ_i varies little as compared to E_C with the increase in j , at least under the conditions considered in this work.

III. MODEL RESULTS AND DISCUSSION

Atmospheric pressure air glow discharges between metallic electrodes and Cu cathodes and for discharge lengths from 0 to 10 mm have been studied in a number of experiments.^{1,2,23–26} The glow-to-arc transition was also investigated in Refs. 23 and 24 in the current range of 10 mA–1 A. It was found that the (sharp) glow-to-arc transition in Cu cathodes occurs at current >0.2 A. Current density data at the cathode are only available for the glow discharge regime (~1–100 mA). Spot current densities for arcs reported by different authors in Cu cathodes lie in the wide range of 10^4 – 10^8 A/cm².^{2,4,27}

Figures 1 and 2 show the axial distributions of the main cathode-sheath parameters, calculated for a current density of 6 A/cm².

Axial profiles of the voltage and electric field are presented in Fig. 1. In order to test the influence of the cathode temperature on the calculated parameters, calculations for a cathode spot at room temperature ($T = 300$ K) are also presented in Fig. 1. It is shown that the cathode temperature influences significantly the main parameters (field distribution, thickness, and voltage drop) of the cathode sheath.

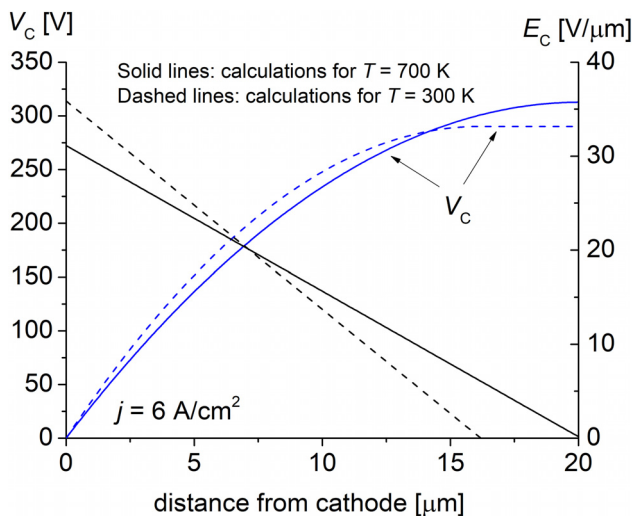


FIG. 1. Axial profiles of the voltage and electric field calculated for a current density of 6 A/cm². For comparative purposes, the same profiles but calculated for a cathode temperature equal to room temperature (300 K) are also shown.

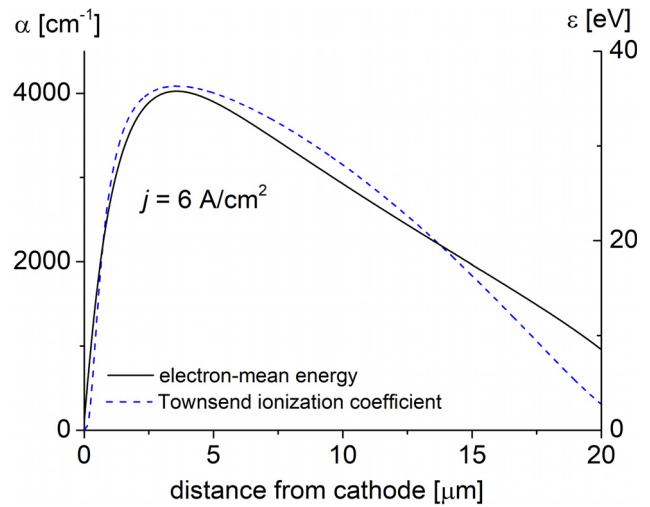


FIG. 2. Axial profiles of the mean electron energy and Townsend ionization coefficient calculated for a current density of 6 A/cm².

In particular, the model predicts an increase in the voltage and thickness of the cathode sheath for a given current density, with increasing cathode spot temperature. These results are consistent with those obtained in a number of investigations.^{28–30} The calculated cathode-sheath voltage (about 313 V) is also in good agreement with zero-length voltage values inferred from voltage measurements under similar conditions.^{1,23–25} The high-voltage drop in the cathode sheath of a glow discharge ensures self-sustenance of plasma by multiple ionization collisions of electrons produced by secondary electron emission.

Axial profiles of the Townsend ionization coefficient and mean electron energy are given in Fig. 2. It is seen that while the electric field decreases over the width of the cathode sheath, both the mean electron energy and the ionization coefficient increase. The reason is that the electrons are accelerated by the field, thus acquiring enough energy for significant ionization only after a given distance from the cathode. The mean electron energy rises rapidly from 1 eV at the cathode surface and reaches its maximum of 36 eV at around 3.5 μm, before decreasing toward the cathode-sheath edge. However, in spite of the fact that the field is very small there, the mean electron energy is still large (around 8 eV) due to the considerable electron acceleration that occurs in the cathode sheath. This means that the ionization is non-local in the cathode sheath (note that the local field approximation would underestimate the ionization coefficient near the plasma boundary and overestimate it near the cathode surface). The spatial variation of the Townsend ionization coefficient emulates that of the mean electron energy, thus suggesting a rapid acceleration of ionization processes therein, to ensure the current continuity through the cathode–gas interface for conditions in which the electron emission is practically absent. The field emission does not play any role under these conditions (as shown in Fig. 5).

Figure 3 shows the same cathode-sheath parameters as Fig. 2 but for an increased current density of $j = 100$ A/cm². It is seen that the mean electron energy increases rapidly from 1 eV at the cathode surface and reaches its maximum of about 40 eV at around 1.8 μm from the cathode. The maximum value of the mean electron energy,

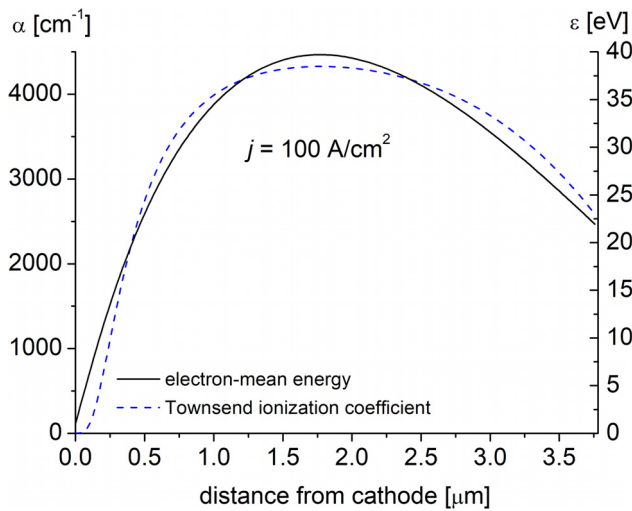


FIG. 3. Axial profiles of the mean electron energy and Townsend ionization coefficient calculated for a current density of 10^2 A/cm².

however, is not far from the cathode-sheath voltage (estimated from Fig. 6 to be only 100 V). This is because very strong ionization is not required as the field emission mechanism is strong enough (see Fig. 5) to provide a significant part of the current to the discharge. The fraction of the electron current at cathode $S [\equiv j_e(0)/j]$ is in this case around 0.3, that is, considerably larger than for glow discharges [$S = \gamma / (1 + \gamma)$] but lower than for arcs ($S \geq 0.6$).⁴ This suggests that this regime corresponds to the early stages of the arcing transition due to field emission. Note that the discharge current density is still well below the values expected for (hot) arc spots on Cu cathodes ($\sim 10^4$ – 10^8 A/cm²).^{4,27} Conditions that prevail within the hot arc spot and that allow such high current densities cannot be described by this model.

The current density dependence of the main parameters of the cathode sheath is given in Figs. 4–6.

Figure 4 shows a rapid increase in the positive space-charge density with the increase in current density, and, according to Poisson's equation, this implies that the spatial derivative of the electric field also grows. This is consistent with the reduction in the thickness of the cathode sheath with the increase in the current density.

Calculations show that the N_2^+ ion is the dominating sort of ion under the high-field conditions considered, with a mole fraction around 0.9, almost independent of the current density value. The reason is that N_2 molecules are more intensively ionized than the O_2 molecules under high-field conditions. The fraction of the electron current at the cathode along with the cathode field is shown in Fig. 5. It is observed that the cathode field increases with current density. With an increase in the electric field, the electrons emitted by the cathode by secondary emission gain more energy and are, in turn, capable of producing more additional electrons through direct ionization. The combination of a larger electric field and a larger number of additional electrons results in a higher current density. This is characteristic of an ionization-dominated cathode sheath and explains the dependence of the cathode electric field on current density in the range of 1–10 A/cm². Any posterior growth in the current density

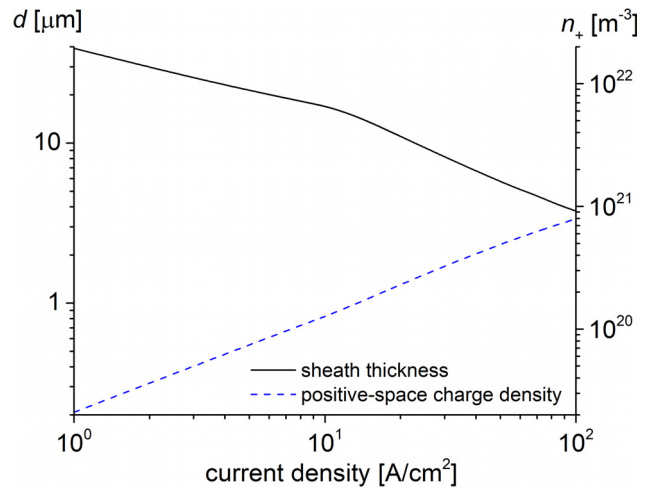


FIG. 4. Current density dependence of the thickness and space-charge density.

above the critical value of ~ 10 A/cm², i.e., for which the field exceeds a critical value of about 45 V/μm, produces a sharp growth of the electron field emission. Multiple ionization collisions are, thus, not required, and the cathode-sheath becomes field emission-dominated. This behavior is seen in Fig. 5 as a change in the slope of the cathode field curve at the critical value of ~ 10 A/cm² and is also consistent with the change in the sign of the slope of the voltage–current density curve (shown in Fig. 6).

Figure 6 highlights three important phases of a typical self-sustained discharge, namely, I—the normal glow discharge when the current density is less than 6 A/cm², II—the abnormal glow discharge phase when the cathode voltage increases monotonically for current densities in the range of ~ 6 A/cm² $< j < 10$ A/cm², and III—the early stages of the arcing transition when the cathode-sheath voltage decreases rapidly for current densities larger than ~ 10 A/cm².

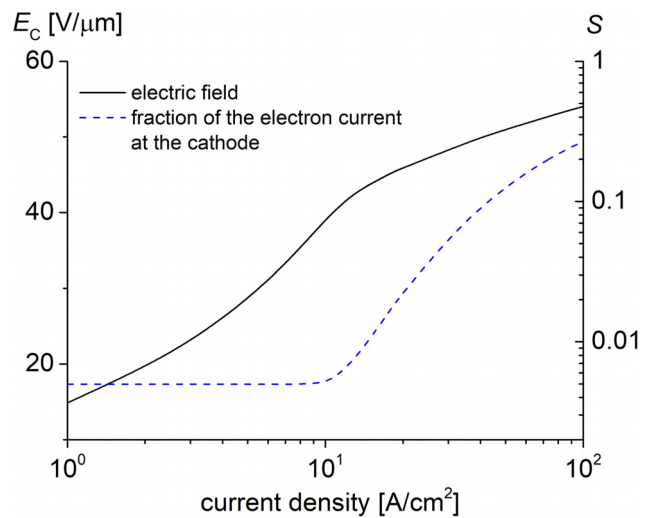


FIG. 5. Current density dependence of the cathode field and fraction of the electron current at the cathode.

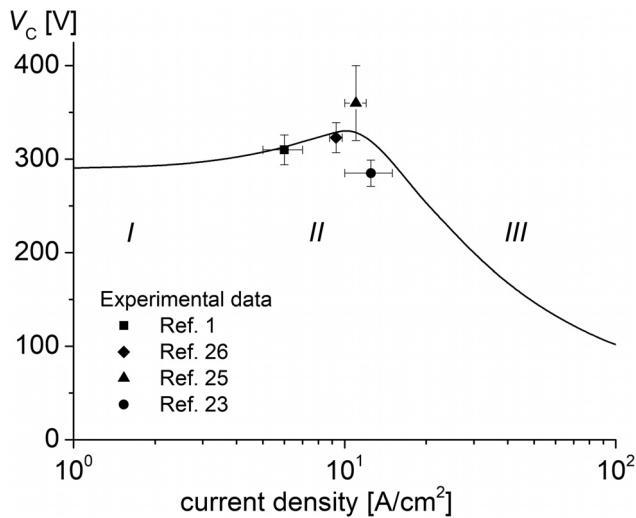


FIG. 6. Voltage–current density characteristic curve. I—the normal glow discharge, II—the abnormal glow discharge, and III—the early stages of the arcing transition.

Although the contraction of glow discharges is often referred to as arcing, the filament plasma regime lies between the non-equilibrium plasma of a glow discharge and the typical equilibrium plasma of thermal arc discharges. The current density in a filament plasma is greater than that in the glow discharge but lower than that in the arc.⁴

Experimental data are also shown in Fig. 6. As can be seen in Fig. 6, the agreement between the model and the available data is good. Note from (4) that the field enhancement factor β has a strong effect on the determination of the critical field (or current density) for the glow-to-arc transition. A change in the value of β shifts the critical current density at which the slope of the curve changes. However, the experimental observation that the glow-to-arc transition occurs at currents >0.2 A,^{23,24} which corresponds to a cathode current density around 10–12 A/cm²,^{24,25} adds confidence on the characteristic curve presented in Fig. 6.

The average number of ion collisions in the cathode sheath is at least one order of magnitude larger than unity over the entire current density range, thus showing that the hydrodynamic description is well justified for ions. This assumption is also justified for electrons since the average number of electron collisions in the cathode sheath is at least comparable to unity, rather than smaller.

IV. CONCLUSIONS

The described model represents a framework to obtain the current density–voltage characteristics of the cathode sheath for a high-pressure discharge in air with a cold cathode. Numerical results were presented in a wide current density range from 1 to 10² A/cm². The proposed model is validated by comparing the numerical results with available experimental data, and a good agreement is found. The main findings are summarized below:

1. The model predicts three important phases of a typical self-sustained discharge: the normal glow discharge, the abnormal glow discharge, and the transition to arcing.
2. The glow-to-arc transition arises from the field-emission instability when the current density is larger than about 10 A/cm²,

i.e., when the cathode field exceeds a critical value of about 45 V/ μ m.

3. The influence of the cathode temperature on the cathode-sheath parameters should be considered in high-pressure discharges.

ACKNOWLEDGMENTS

This work was supported by grants from the Universidad Tecnológica Nacional (PID 5447 and PID 5418) and Agencia Nacional de Promoción Científica y Tecnológica (Grant No. PICT 2015-1553). L.P., F.O.M., and B.F. are members of the CONICET. E.C. and M.F. thank CONICET for their doctoral fellowships. J.C.C. thanks CONICET for his postdoctoral fellowship.

DATA AVAILABILITY

The data that support the findings of this study are available within this article.

REFERENCES

- ¹D. Staack, B. Farouk, A. Gutsol, and A. Fridman, *Plasma Sources Sci. Technol.* **14**, 700 (2005).
- ²D. Staack, B. Farouk, A. Gutsol, and A. Fridman, *Plasma Sources Sci. Technol.* **17**, 025013 (2008).
- ³E. E. Kunhardt, *IEEE Trans. Plasma Sci.* **28**, 189 (2000).
- ⁴Y. P. Raizer, *Gas Discharge Physics* (Springer-Verlag, Berlin, 1991), pp. 167–285.
- ⁵M. Cernak, T. Hoder, and Z. Bonaventura, *Plasma Sources Sci. Technol.* **29**, 013001 (2020).
- ⁶W. S. Boyle and F. E. Haworth, *Phys. Rev.* **101**, 935 (1956).
- ⁷D. B. Go and A. Venkattraman, *J. Phys. D* **47**, 503001 (2014).
- ⁸S. S. Tholeti, A. Semnani, D. Peroulis, and A. A. Alexeenko, *Phys. Plasmas* **22**, 083508 (2015).
- ⁹Yu. Akishev, V. Karalnik, I. Kochetov, A. Napartovich, and N. Trushkin, *Plasma Sources Sci. Technol.* **23**, 054013 (2014).
- ¹⁰D. Spasojevic, V. Steflelova, N. M. Sisovic, and N. Konjevic, *Plasma Sources Sci. Technol.* **21**, 025006 (2012).
- ¹¹T. N. An, E. Marode, and P. C. Johnson, *J. Phys. D* **10**, 2317 (1977).
- ¹²L. A. Viehland and E. A. Mason, *At. Data Nucl. Data Tables* **60**, 37 (1995).
- ¹³E. Levin and M. J. Wright, *J. Thermophys. Heat Transfer* **18**, 143 (2004).
- ¹⁴R. F. Stebbings, B. R. Turner, and A. C. H. Smith, *J. Chem. Phys.* **38**, 2277 (1963).
- ¹⁵R. H. Fowler and L. W. Nordheim, *Philos. Trans. R. Soc. London* **119**, 173 (1928).
- ¹⁶R. E. Burgess, H. Kroemer, and J. M. Houston, *Phys. Rev.* **90**, 515 (1953).
- ¹⁷A. A. Kudryavtsev, A. V. Morin, and L. D. Tsendin, *Tech. Phys.* **53**, 1029 (2008).
- ¹⁸J. J. Shi and M. G. Kong, *J. Appl. Phys.* **94**, 5504 (2003).
- ¹⁹G. J. M. Hagelaar and L. C. Pitchford, *Plasma Sources Sci. Technol.* **14**, 722 (2005).
- ²⁰See <http://www.lxcat.laplace.univ-tlse.fr> for “SIGLO Database” (last accessed June 4, 2013).
- ²¹J. P. Boeuf and L. C. Pitchford, *Phys. Rev. E* **51**, 1376 (1995).
- ²²E. Eylenceoglu, I. Rafatov, and A. A. Kudryavtsev, *Phys. Plasmas* **22**, 013509 (2015).
- ²³W. A. Gambling and H. Edels, *Br. J. Appl. Phys.* **5**, 36 (1954).
- ²⁴W. A. Gambling, *Stud. Q. J.* **24**, 15 (1953).
- ²⁵L. Prevosto, H. Kelly, B. Mancinelli, J. C. Chamorro, and E. Cejas, *Phys. Plasmas* **22**, 023504 (2015).
- ²⁶P. Mezei, T. Cserfalvi, and M. Janossy, *J. Phys. D* **34**, 1914 (2001).
- ²⁷I. I. Beilis, *IEEE Trans. Plasma Sci.* **47**, 3412 (2019).
- ²⁸I. Revel, L. C. Pitchford, and J. P. Boeuf, *J. Appl. Phys.* **88**, 2234 (2000).
- ²⁹A. Bogaerts and R. Gijbels, *J. Appl. Phys.* **87**, 8334 (2000).
- ³⁰V. I. Arkhipenko, A. A. Kirillov, Y. A. Safronau, L. V. Simonchik, and S. M. Zgirouski, *Plasma Sources Sci. Technol.* **17**, 045017 (2008).